- Collective Conformations of DNA Polymers Assembled on Surface Density Gradients
  Shemer, G.; Atsmon, A.; Karzbrun, E.; Bar-Ziv, R. H. *J. Am. Chem. Soc.* **2012**, *134*, 3954–3956.
  Abstract:

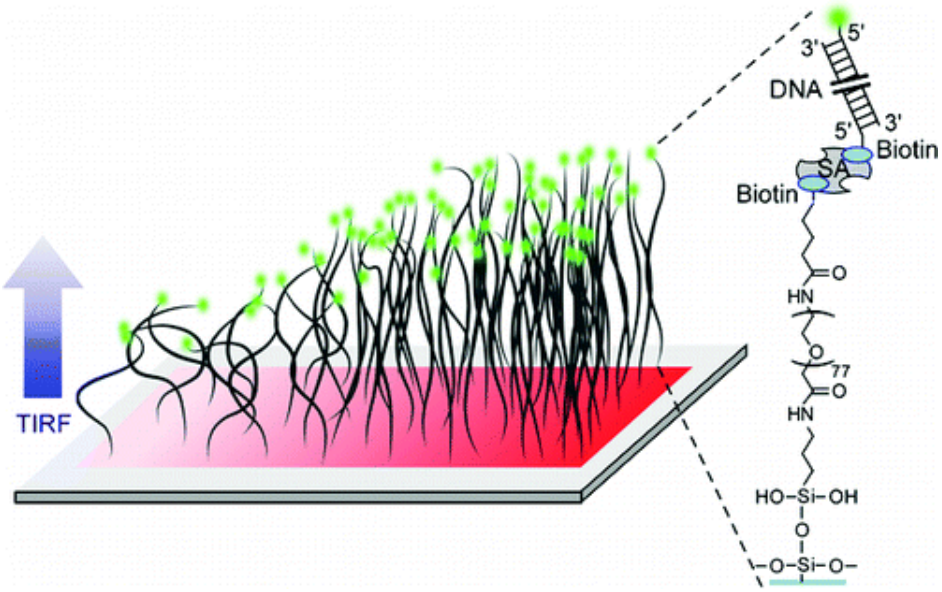

To study dense double-stranded DNA (dsDNA) polymer phases, we fabricated continuous density gradients of binding sites for assembly on a photochemical interface and measured both dsDNA occupancy and extension using evanescent fluorescence. Despite the abundance of available binding sites, the dsDNA density saturates after occupation of only a fraction of the available sites along the gradient. The spatial position at which the density saturates marks the onset of collective stretching of dsDNA, a direct manifestation of balancing entropic and excluded-volume interactions. The methodology presented here offers a new means to investigate dense dsDNA compartments.

- Glycopolypeptides with a Redox-Triggered Helix-to-Coil Transition
  Kramer, J. R.; Deming, T. J. *J. Am. Chem. Soc.* **2012**, *134*, 4112–4115.
  Abstract:

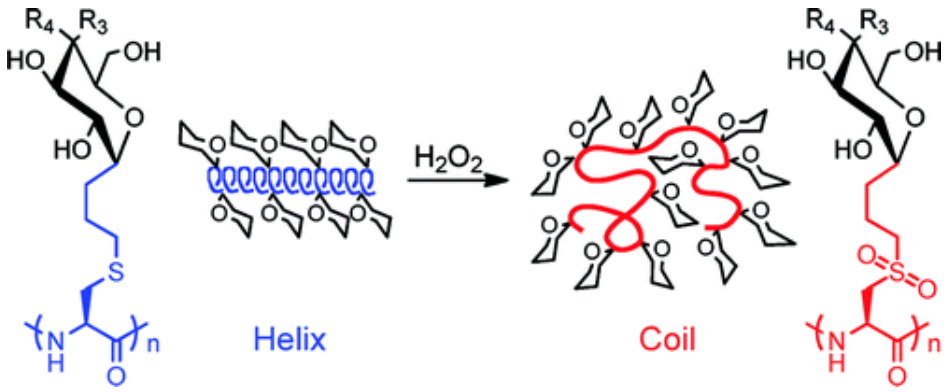

Conformation-switchable glycopolypeptides were prepared by the living polymerization of glycosylated l-cysteine-*N*-carboxyanhydride (glyco-C NCA) monomers. These new monomers were prepared in high yield by coupling of alkene-terminated C-linked glycosides of d-galactose or d-glucose to l-cysteine using thiol–ene “click” chemistry, followed by their conversion to the corresponding glyco-C NCAs. The resulting glycopolypeptides were found to be water-soluble and α-helical in solution. Aqueous oxidation of the side-chain thioether linkages in these polymers to sulfone groups resulted in disruption of the α-helical conformations without loss of water solubility.

The ability to switch chain conformation and remain water-soluble is unprecedented in synthetic polymers, and allows new capabilities to control presentation of sugar functionality in subtly different contexts.

- Up to 4 Orders of Magnitude Enhancement of Crown Ether Complexation in an Aqueous Phase Coexistent with Ice
  Tasaki, Y.; Okada, T. *J. Am. Chem. Soc.* **2012**, *134*, 6128–6131.
  Abstract:

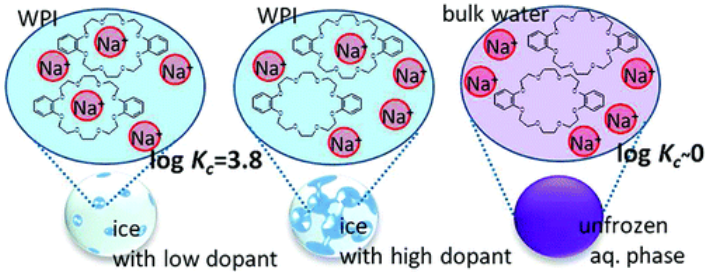

Ice chromatography measurements have revealed anomalous enhancements of crown ether complexation in a liquid phase coexistent with ice. The 4 orders of magnitude enhancement was confirmed for the complexation of dibenzo-24-crown-8 in sub-µm-sized liquid inclusions formed in ice doped with <1 mM NaCl or KCl. This enhancement became less pronounced with increasing dopant concentration.

- Enhanced Epimerization of Glycosylated Amino Acids During Solid-Phase Peptide Synthesis
  Zhang, Y.; Muthana, S. M.; Farnsworth, D.; Ludek, O.; Adams, K.; Barchi, Jr., J. J.; Gildersleeve, J. C. *J. Am. Chem. Soc.* **2012**, *134*, 6316–6325.
  Abstract:

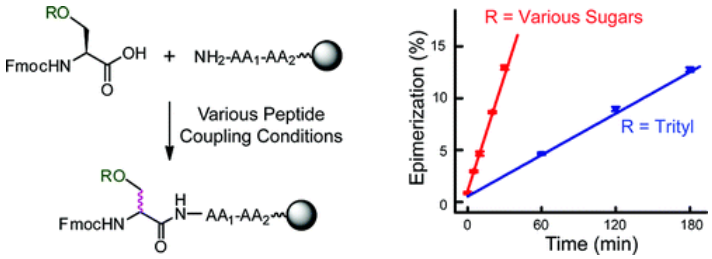

Glycopeptides are extremely useful for basic research and clinical applications, but access to structurally defined glycopeptides is limited by the difficulties in synthesizing this class of compounds. In this study, we demonstrate that many common peptide coupling conditions used to prepare *O*-linked glycopeptides result in substantial amounts of epimerization at the α position. In fact, epimerization resulted in up to 80% of the non-natural epimer, indicating that it can be the major product in some reactions. Through a series of mechanistic studies, we demonstrate that the enhanced epimerization relative to nonglycosylated amino acids is due to a combination of factors, including a faster rate of epimerization, an energetic preference for the unnatural epimer over the natural epimer, and a slower overall rate of peptide coupling. In addition, we demonstrate that use of 2,4,6-trimethylpyridine (TMP) as the base in peptide couplings produces glycopeptides with high efficiency and low epimerization. The information and improved reaction conditions will facilitate the preparation of glycopeptides as therapeutic compounds and vaccine antigens.

- Design and characterization of alkoxy-wrapped push–pull porphyrins for dye-sensitized solar cells
  Sanchis, T. R.; Guo, B. C.; Wu, H. P.; Pan, T. Y.; Lee, H. W.; Raga, S. R.; Santiago, R. R.; Bisquert, J.; Yeh, C. Y.; Diau, E. W. G. *Chem. Commun.* **2012**, *48*, 4368-4370.
  Abstract:

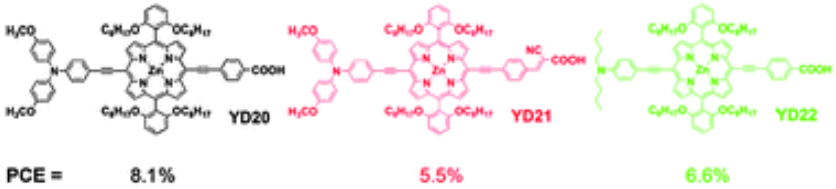

Porphyrins YD20–YD22 are synthesized and characterized to provide evidence for the device performances in relation to their structural and charge recombination features.

- Solvent-dependent amplification of chirality in assemblies of porphyrin trimers based on benzene tricarboxamide
  Veling, N.; Hameren, R.; Buul, A. M.; Rowan, A. E.; Nolte, R. J. M.; Elemans J. A. A. W. *Chem. Commun.* **2012**, *48*, 4371-4373.
  Abstract:

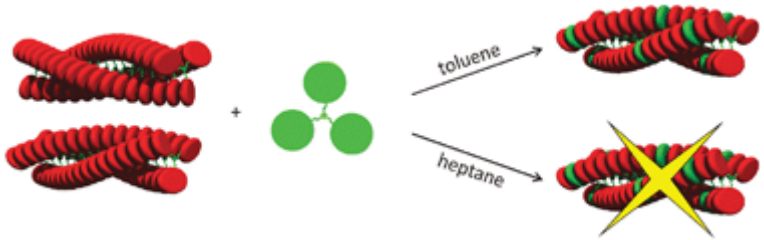

Self-assembling achiral and chiral porphyrin trimers exhibit amplification of chirality only in solvents where dynamic exchange of their components occurs.

- Macrocyclic depolymerization of arylene-ethynylene copolymers: a dynamic combinatorial method
  Gross , D. E.; Discekici, E.; Moore, J. S. *Chem. Commun.* **2012**, *48*, 4426-4428.
  Abstract:

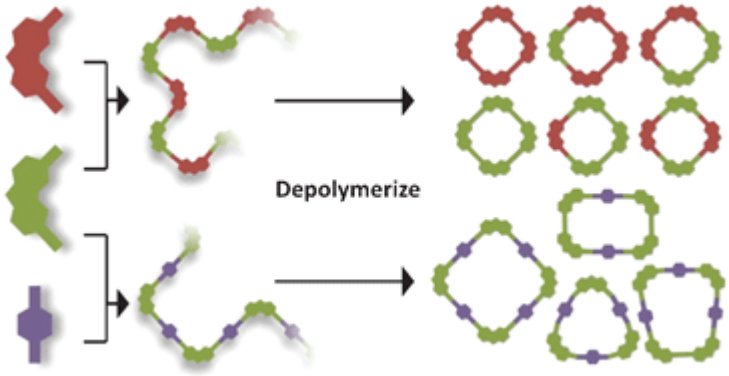

A dynamic combinatorial approach for the synthesis of arylene ethynylene macrocycles (AEMs) from linear polymers is described. By using readily available carbazolyl-ethynylene copolymers as starting materials we obtained a number of novel macrocycles that would be difficult to prepare by traditional methods.

- Preparation and structural control of metal coordination-assisted supramolecular architectures of porphyrins. Nanocubes to microrods
  Sakuma, T.; Sakai, H.; Hasobe, T. *Chem. Commun.* **2012**, *48*, 4441-4443.
  Abstract:

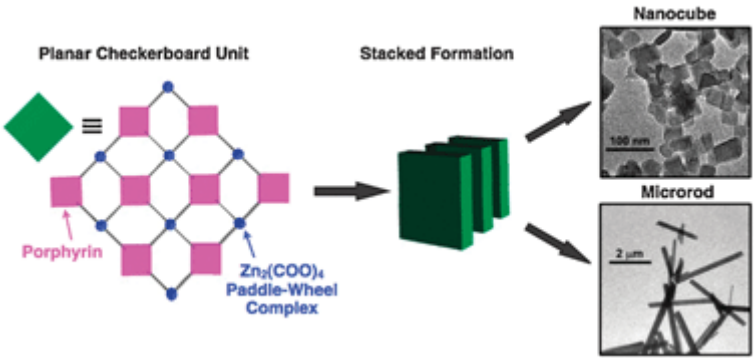

We have successfully prepared metal coordination-assisted porphyrin assemblies such as nanocubes, nanorods and microrods by controlling the synthetic conditions. The internal structures and lifetimes of the excited states are also quantitatively discussed.

- Metallosupramolecular amphiphilic π-systems
  Muñoz, M. J. M.; Fernández, G. *Chem. Sci.* **2012**, *3*, 1395-1398.
  Abstract:

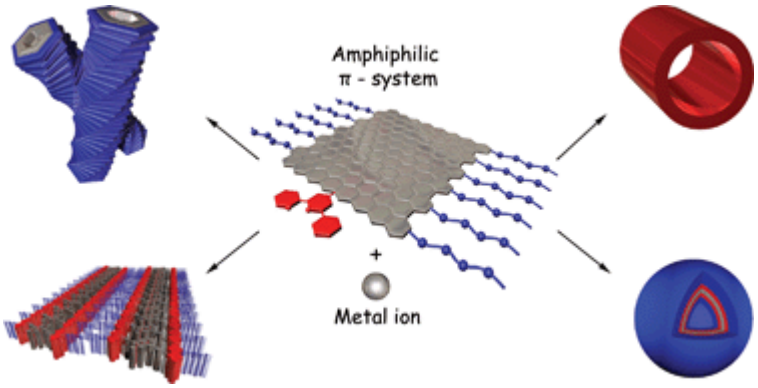

Metallosupramolecular π-amphiphiles are emerging as a new class of adaptive materials with the ability to self-assemble into a wide variety of supramolecular structures through simultaneous π-π, metallophilic and metal-ligand interactions.

- Development of a robust supramolecular method to prepare well-defined nanofibrils from conjugated molecules
  Tian, L.; Szilluweit, R.; Marty, R.; Bertschi, L.; Zerson, M.; Spitzner, E. C.; Magerle, R.; Frauenrath, H. *Chem. Sci.* **2012**, *3*, 1512-1521.
  Abstract:

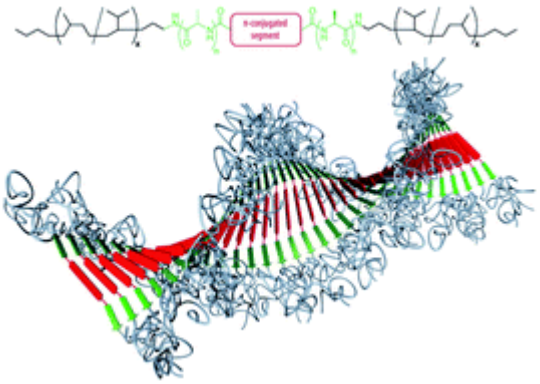

Oligopeptide–polymer derivatives comprising a flexible polymer segment terminally attached to a β-sheet-forming oligopeptide segment are simple substituents that suppress lateral aggregation, promote one-dimensional aggregation, and are compatible with productive π–π overlap of the constituting molecules.

- Redox-Gated Potential Micellar Carriers Based on Electrostatic Assembly of Soft Coordination Suprapolymers
  Zhao, L.; Yan, Y.; Huang, J. *Langmuir* **2012**, *28*, 5548–5554.
  Abstract:

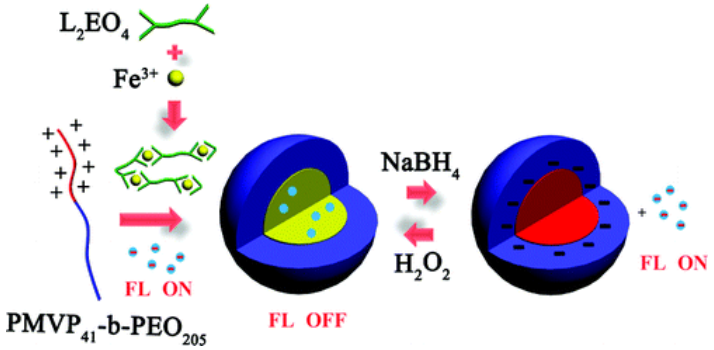

We report in this paper the release and uptake of charged payloads in redox responsive electrostatic micellar systems composed of negatively charged soft iron coordination suprapolymers and positively charged block copolymers. This micellar system was reported in our previous work (Yan, Y.; Lan, Y. R.; de Keizer, A.; Drechsler, M.; Van As, H.; Stuart, M. A. C.; Besseling, N. A. M. Redox responsive molecular assemblies based on metallic coordination polymers. *Soft Matter*, **2010**, *6*, 3244–3248), where we proposed that the system can be used as a redox-triggered release and uptake system. In this paper, we successfully selected a negatively charged fluorescent dye, eosin B, as a model cargo to track the release and upload process. Upon being compacted in the mixed micelles of coordination polymers and diblock copolymers, the fluorescence of eosin B was effectively quenched. Once reduction was conducted, excess negative charges were introduced to the mixed micelles so that the negatively charged eosin B was expelled out which was accompanied by the recovery of the fluorescence. The free negatively charged eosin B was able to be taken up by the Fe(II) micelles again if oxidation of Fe(II) was carried out since excess positive charges were produced. Beside eosin B, other charged species, such as various charged macromolecules, were tested to be capable of uptake and release by this micellar system. We suppose this system can be potentially used as a redox-gated micellar carrier for uptake and release of charged cargos.

- Design and Fabrication of Gecko-Inspired Adhesives

Jin, K.; Tian, Y.; Erickson, J. S.; Puthoff, J.; Autumn, K.; Pesika, N. S. *Langmuir* **2012**, *28*, 5737-5742.

Abstract:

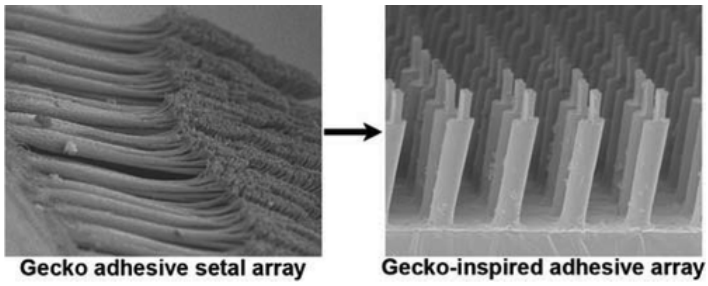

Recently, there has been significant interest in developing dry adhesives mimicking the gecko adhesive system, which offers several advantages compared to conventional pressure-sensitive adhesives. Specifically, gecko adhesive pads have anisotropic adhesion properties; the adhesive pads (spatulae) stick strongly when sheared in one direction but are non-adherent when sheared in the opposite direction. This anisotropy property is attributed to the complex topography of the array of fine tilted and curved columnar structures (setae) that bear the spatulae. In this study, we present an easy, scalable method, relying on conventional and unconventional techniques, to incorporate tilt in the fabrication of synthetic polymer-based dry adhesives mimicking the gecko adhesive system, which provides anisotropic adhesion properties. We measured the anisotropic adhesion and friction properties of samples with various tilt angles to test the validity of a nanoscale tape-peeling model of spatular function. Consistent with the peel zone model, samples with lower tilt angles yielded larger adhesion forces. The tribological properties of the synthetic arrays were highly anisotropic, reminiscent of the frictional adhesion behavior of gecko setal arrays. When a 60° tilt sample was actuated in the gripping direction, a static adhesion strength of ~1.4 N/cm^2 and a static friction strength of ~5.4 N/cm^2 were obtained. In contrast, when the dry adhesive was actuated in the releasing direction, we measured an initial repulsive normal force and negligible friction.

- A New Supramolecular Hole Injection/Transport Material on Conducting Polymer for Application in Light-Emitting Diodes
  Chu, Y.-L.; Cheng, C.-C.; Yen, Y.-C.; Chang, F. C. *Adv. Mater.* **2012**, 24, 1894–1898.
  Abstract:

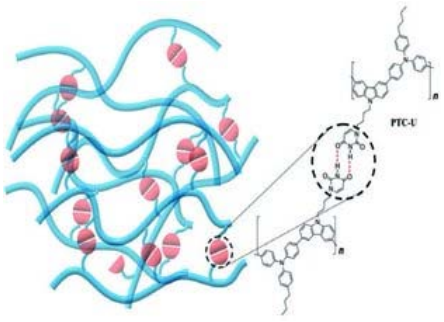

A new DNA-mimetic π-conjugated polymer poly(triphenylamine-carbazole) (PTC-U) has been prepared which exhibits high thermal stability, non-corrosion, excellent hole injection and electron-blocking abilities in the solid state owing to the uracil induced physical cross-linking. In addition, a trilayer device with PTC-U as a hole injection/transport layer is approximately 1.6 times higher than that of the commercial product PEDOT:PSS-based devices.

- Small-Molecule Photovoltaics Based on Functionalized Squaraine Donor Blends
  Xiao, X.; Wei, G.; Wang, S.; Zimmerman, J. D.; Renshaw, C. K.; Thompson, M. E.; Forrest, S. R. *Adv. Mater.* **2012**, *24*, 1956–1960.
  Abstract:

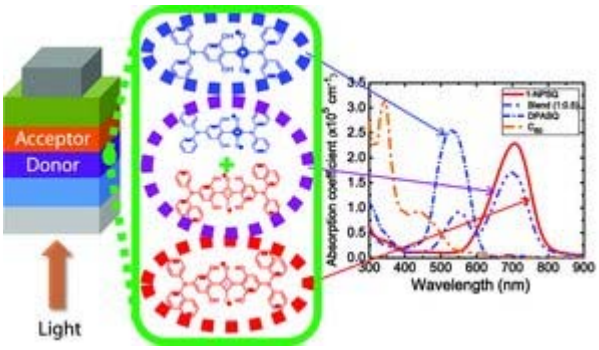

Two squaraine (SQ) donor molecules with different absorption bands are blended together for better coverage of the solar spectrum. The blend SQ device shows a significant improvement compared with single SQ donor devices. By applying a solvent annealing process and a compound buffer layer, a power-conversion efficiency of 5.9 ± 0.3% is achieved under 1 sun illumination.

- Cooperative Assembly of Hydrogen-Bonded Diblock Copolythiophene/Fullerene Blends for Photovoltaic Devices with Well-Defined Morphologies and Enhanced Stability
  Lin, Y.; Lim, J. A.; Wei, Q.; Mannsfeld, S. C. B.; Briseno, A. L.; Watkins, J. J. *Chem. Mater.* **2012**, *24*, 622–632.
  Abstract:

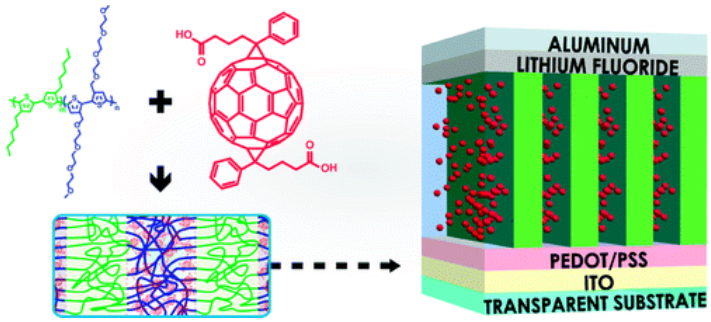

We report the cooperative self-assembly of functionalized fullerenes and all conjugated block copolymers (BCPs) containing polythiophene derivatives in both segments to yield solar cells with well-defined nanostructures and enhanced morphological stability. Favorable hydrogen bonding interactions between the COOH-functionalized fullerene, bis-[6, 6]-phenyl C61-butyric acid (bis-PCBA), and the tetraethyleneglycol side chains of poly(3-hexylthiophene)-*block*-poly[3-(2,5,8,11-tetraoxadodecane)thiophene] (P3HT-*b*-P3TODT) allows for high loading of bis-PCBA (up to 40 wt % to the blend) within the P3TODT domains, while preserving the lamellar morphology. Characterization by grazing incidence small-angle X-ray scattering, electron microscopy, and atomic force microscopy indicates that the periods of the structures range between 24 and 29 nm depending on the bis-PCBA loading. The hydrogen bond interactions between bis-PCBA and P3TODT segments further suppress crystallization and macrophase separation of the fullerenes, even under harsh annealing conditions (150 °C for 12 h). Bulk heterojunction solar cells prepared using P3HT-*b*-P3TODT/bis-PCBA exhibit a photoconversion efficiency of 2.04%, which is greater than that of a reference system, P3HT-*b*-P3TODT/bis-PCBM. Accelerated aging experiments reveal enhanced thermal stability as a result of the limited translational mobility of COOH-functionalized fullerene in P3HT-*b*-P3TODT relative to

devices prepared using bis-PCBM in P3HT-*b*-P3TODT or P3HT. We believe that cooperative assembly using strong noncovalent interactions is a general approach that can be used to improve the processing, morphological stability, and aging of organic and hybrid photovoltaic devices.

- Triphenylamine Dendronized Iridium(III) Complexes: Robust Synthesis, Highly Efficient Nondoped Orange Electrophosphorescence and the Structure–Property Relationship
  Zhu, M.; Zou, J.; He, X.; Yang, C.; Wu, H.; Zhong, C.; Qin, J.; Cao, Y. *Chem. Mater.* **2012**, *24*, 174–180.
  Abstract:

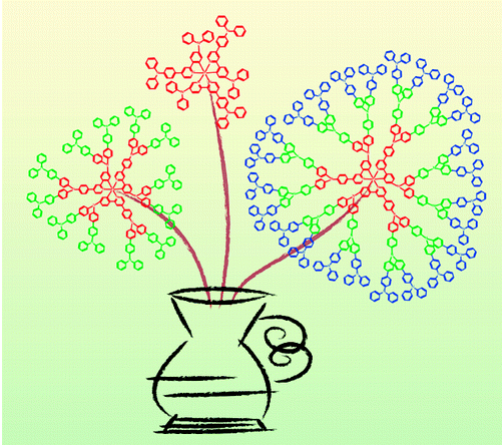

New triphenylamine dendronized homoleptic Ir(III) complexes, namely **Ir-G1**, **Ir-G2**, and **Ir-G3**, with six, eighteen, and up to forty-two triphenylamine units, respectively, are designed and efficiently synthesized through convergent strategy. Both linear enlargement of the dendritic arms and the "double-dendron" strategy are applied to maximize the degree of site-isolation of the emissive center. The relationship between the dendritic structures and their photophysical, electrochemical, and electrophosphorescent performances is investigated. Phosphorescent organic light-emitting diodes (PhOLEDs) employing the dendrimers as solution-processed emitters are fabricated. The nondoped devices with **Ir-G1** and **Ir-G2** as emitters display very high efficiencies and small values of efficiency roll-off. For example, a device with **Ir-G1** as emitter exhibits the best results ever reported for solution-processed orange phosphorescent devices with maximum luminous efficiency of 40.9 cd A^{-1} and power efficiency of 39.5 lm W^{-1}. Moreover, the maximum power efficiency of the nondoped device is nearly three times higher than that of the doped control device by doping **Ir-G1** into the general polymer matrix. This indicates that incorporation of triphenylamine moieties into the sphere of iridium(III) core is a simple and effective approach to develop highly efficient host-free dendritic phosphors.

- Plasmon Shaping by using Protein Nanoarrays and Molecular Lithography to Engineer Structural Color
  Clark, A. W.; Cooper, J. M. *Angew. Chem. Int. Ed.* **2012**, *51*, 3562-3566.
  Abstract:

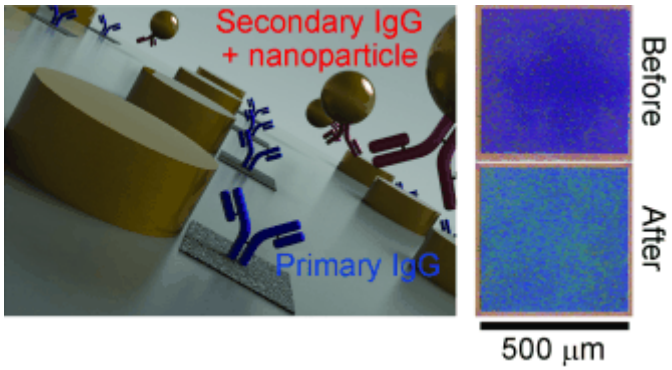

Naked-eye detection: The versatility of direct-write nanolithography was combined with the unrivaled resolution and selectivity of molecular self-assembly to show, for the first time, the molecularly mediated placement, with nanometer accuracy, of single Au nanoparticles within a plasmonic array. In doing so, a coupled plasmonic systems was created which allowed colorimetric, naked-eye detection of protein–protein binding at extreme sensitivities.

- Chemistry at the Nanoscale: Synthesis of an N@C60–N@C60 Endohedral Fullerene Dimer
  Farrington, B. J.; Jevric, M.; Rance, G. A.; Ardavan, A.; Khlobystov, A. N.; Briggs, G. A. D.; Porfyrakis, K. *Angew. Chem. Int. Ed.* **2012**, *51*, 3587-3890.
  Abstract:

Rattling the cage: The rapid one-pot double 1,3-dipolar cycloaddition reaction of the rare endohedral fullerene N@C60 to an oligo(p-phenylene polyethylene) bis(aldehyde) using a novel amino acid derivative as an anchoring group is reported. The method provides the first example of a chemically linked, two-spin-center N@C60–N@C60 molecule (see picture). Assessment of this platform as an element of a quantum computing register is attractive.

- Spirobifluorene-Based Conjugated Polymers for Polymer Solar Cells with High Open-Circuit Voltage
  Wang, M.; Li, C.; Lv, A.; Wang, Z.; Bo, Z. *Macromolecules* **2012**, *45*, 3017–3022.
  Abstract:

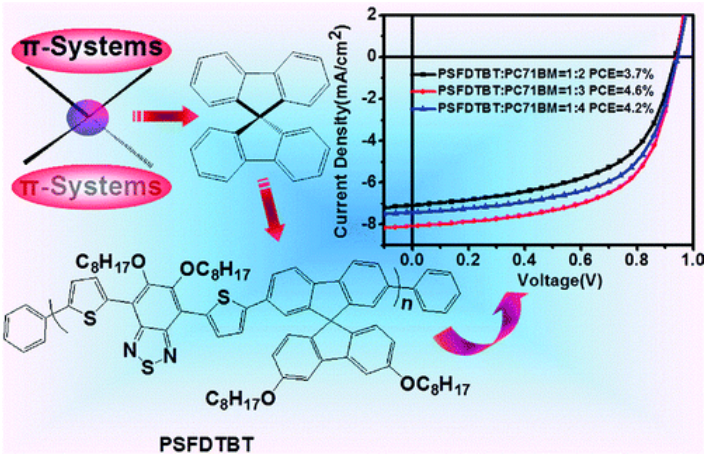

A new alternating copolymer (**PSFDTBT**) based on spirobifluorene, thiophene, and benzothiadiazole units has been synthesized. **PSFDTBT** has an optical band gap of 1.97 eV with the low-lying HOMO energy level at −5.4 eV. The hole mobility of the pristine **PSFDTBT** film spin-cast from *o*-dichlorobenzene (DCB) solution is 7.26×10^{-3} cm^2 V^{-1} s^{-1} with on/off ratios in the order of 10^5. Polymer solar cell devices based on the blend films of **PSFDTBT** and $PC_{71}BM$ show a high open-circuit voltage of 0.94 V and a power conversion efficiency of 4.6% without any post-treatment. All the device measurements were performed in air without encapsulation. This is the first report on spirobifluorene-based conjugated polymers used for polymer solar cells, demonstrating the great potential of spirobifluorene moiety as an electron-donating unit for the construction of main chain donor–acceptor alternating conjugated polymers for high performance polymer solar cells.

- Synthesis and Luminescence of POSS-Containing Perylene Bisimide-Bridged Amphiphilic Polymers
  Du, F.; Tian, J.; Wang, H.; Liu, B.; Jin, B.; Bai, R. *Macromolecules* **2012**, *45*, 3086–3093.
  Abstract:

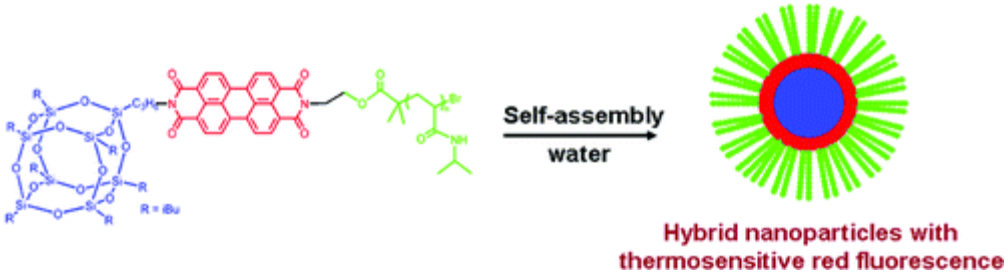

A novel well-defined amphiphilic fluorescent polymer containing asymmetric perylene bisimide was designed and synthesized by combining reaction of perylene anhydride with amino functional polyhedral oligomeric silsesquioxane (POSS) and atom transfer radical polymerization (ATRP) of *N*-isopropylacrylamide (NIPAM). All the intermediate and final products were characterized by NMR, Fourier transform infrared spectroscopy (FT-IR), elemental analyses, and gel permeation chromatograph (GPC). Self-assembly of the amphiphilic polymers was investigated in aqueous solution and POSS-containing hybrid nanoparticles were obtained and characterized by dynamic laser light scattering (DLS) and transmission electron microscopy (TEM). The novel hybrid nanoparticles exhibit attractive high red fluorescence at 645 nm due to the significant effect of the bulky POSS moieties. Moreover, based on the thermoresponsive PNIPAM coronas, the fluorescence intensity of the self-assembled hybrid nanoparticles can be further enhanced and tuned by changing temperature.

- Incorporation of Positively Charged Linkages into DNA and RNA Backbones: A Novel Strategy for Antigene and Antisense Agents
  Jain, M. L.; Bruice, P. Y.; Szabó, I. E.; Bruice, T. C. *Chem. Rev.* **2012**, *112*, 1284-1309.
  Abstract:

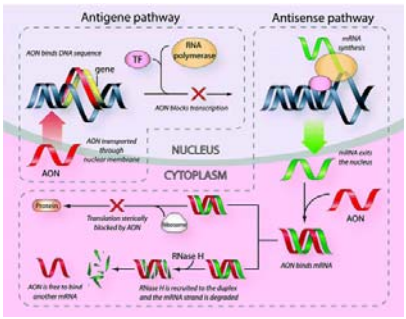

The discovery, in 1978, by Zamecnik and Stephson that an oligonucleotide can inhibit viral replication in cell cultures ushered in an era of antisense therapeutics. After more than 20 years of experimentation, antisense technology led to the commercialization of the first antisense oligonucleotide drug, Fomivirsen, for cytomegalovirus retinitis. Several others are currently in clinical trials for a wide range of human diseases such cancer, AIDS, hepatitis C, solid tumors, asthma, psoriasis, rheumatoid arthritis, cardiovascular disease, and diabetes.

Antigene agents are nucleic acid analogues that function by entering the nucleus of a cell and interfering with the *transcription* of DNA into mRNA (Figure 1). The introduction of a single-stranded antigene agent results in formation of a double-stranded DNA (dsDNA)·antigene triplex that prevents transcription of the target DNA sequence. *Antisense agents* function in the cytoplasm of the cell, where they interfere with the *translation* of mRNA into protein via two common pathways (Figure 1). One pathway involves binding the antisense oligonucleotide to the target mRNA strand, which sterically hinders ribosome binding and therefore mRNA translation. The second pathway involves digestion of the target mRNA by the enzyme RNase H; certain antisense oligonucleotides are adept at recruiting RNase binding to mRNA, facilitating the degradation of the mRNA transcript. In order to be considered effective, antigene/antisense candidates must have a high affinity and specificity for their target DNA or mRNA sequences and must be resistant to degradation by cellular nucleases. The development of antisense/antigene agents should focus on improving the efficacy and drug delivery of these agents, while reducing nonspecific interactions and unwanted side-effects.

- Bioinorganic Chemistry of Titanium
  Buettner, K. M.; Valentine, A. M. *Chem. Rev.* **2012**, *112*, 1863-1881.
  Abstract:

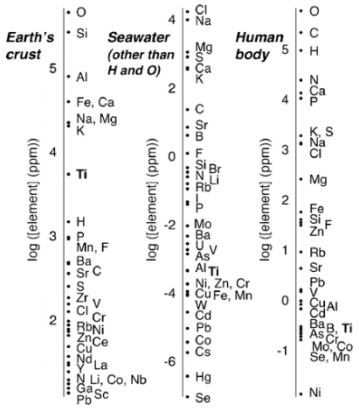

Louis-Camille Maillard is best remembered for his namesake organic reaction, one between an amino acid and a reducing sugar. In his final four papers before his death in 1936, however, Maillard reported on the occurrence and possible role of titanium in mammals, and in particular in humans. In his last paper, Maillard concluded:

"At the present time, nothing allows us to say whether titanium must be regarded as a constitutional element of the human material, or an accidental one, and we intend for the moment not to take sides, either in one direction or in the other. For this reason, we prefer to declare [that titanium is] not a new element *of* the human body, but more modestly, a new element *in* the human body."
Seventy-five years later, conventional wisdom in bioinorganic chemistry still holds that there is no native role for Ti in the biology of any organism, much less that of humans. Some reports in the literature across several fields suggest that Ti is biologically active, however, and this review attempts to bring together these pieces into a coherent whole, so that the role of Ti as a biological element can better be considered.
Inorganic elements in biology include those with some natural biological effect, whether beneficial or harmful, as well as those used medicinally as probes or drugs. The beneficial members of the former group include widely employed elements (such as iron, copper, and zinc) as well as elements that are used by just a few species (such as cadmium and tungsten). When we consider which inorganic elements Nature has selected through evolution, we generally say that Nature employs elements that (1) facilitate useful chemistry and (2) are sufficiently abundant and sufficiently bioavailable for organisms to benefit from their exploitation. Given these selection criteria, it would be surprising if Ti were not a biological element. Humans have found numerous uses for Ti, including in its complexed form as a catalyst in many important transformations, in its oxide form as a pigment and a component of promising solar cells, and in its oxide or alloy forms as useful materials. If Ti has no native role in biology, then humans have found valuable applications for an element for which Nature has never found a use.

- Small-molecule inhibitors of the AAA1 ATPase motor cytoplasmic dynein
  Firestone, A. J.; Weinger, J. S.; Maldonado, M.; Barlan, K.; Langston, L. D.; O'Donnell, M.; Gelfand, V. I.; Kapoor, T. M.; Chen, J. K. *Nature* **2012**, *484*,125-129.
  Abstract:

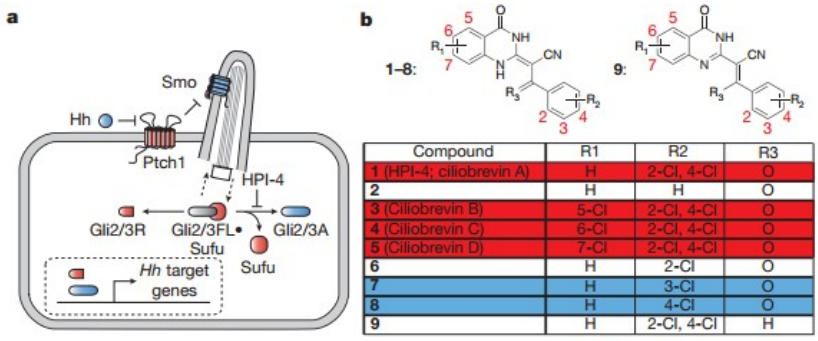

Compound	R1	R2	R3
1 (HPI-4; ciliobrevin A)	H	2-Cl, 4-Cl	O
2	H	H	O
3 (Ciliobrevin B)	5-Cl	2-Cl, 4-Cl	O
4 (Ciliobrevin C)	6-Cl	2-Cl, 4-Cl	O
5 (Ciliobrevin D)	7-Cl	2-Cl, 4-Cl	O
6	H	2-Cl	O
7	H	3-Cl	O
8	H	4-Cl	O
9	H	2-Cl, 4-Cl	H

The conversion of chemical energy into mechanical force by AAA+ (ATPases associated with diverse cellular activities) ATPases is integral to cellular processes, including DNA replication, protein unfolding, cargo transport and membrane fusion. The AAA+ ATPase motor cytoplasmic dynein regulates ciliary trafficking, mitotic spindle formation and organelle transport, and dissecting its precise functions has been challenging because of its rapid timescale of action and the lack of cell-permeable, chemical modulators. Here we describe the discovery of ciliobrevins, the first specific small-molecule antagonists of cytoplasmic dynein. Ciliobrevins perturb protein trafficking within the primary cilium, leading to their malformation and Hedgehog signalling blockade. Ciliobrevins also prevent spindle pole focusing, kinetochore-microtubule attachment, melanosome aggregation and peroxisome motility in cultured cells. We further demonstrate the ability of ciliobrevins to block dynein-dependent microtubule gliding and ATPase activity in vitro. Ciliobrevins therefore will be

useful reagents for studying cellular processes that require this microtubule motor and may guide the development of additional AAA+ ATPase superfamily inhibitors.

- High-Resolution EM of Colloidal Nanocrystal Growth Using Graphene Liquid Cells
  Yuk, J. M.; Park, J.; Ercius, P.; Kim, K.; Hellebusch, D. J.; Crommie, M. F.; Lee, J. Y.; Zettl, A.; Alivisatos, A. P. *Science* **2012***, 336*, 61-64.
  Abstract:

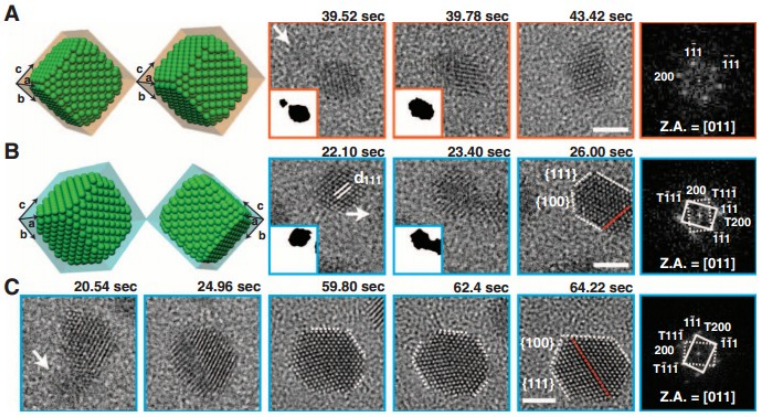

We introduce a new type of liquid cell for in situ transmission electron microscopy (TEM) based on entrapment of a liquid film between layers of graphene. The graphene liquid cell facilitates atomic-level resolution imaging while sustaining the most realistic liquid conditions achievable under electron-beam radiation. We employ this cell to explore the mechanism of colloidal platinum nanocrystal growth. Direct atomic-resolution imaging allows us to visualize critical steps in the process, including site-selective coalescence, structural reshaping after coalescence, and surface faceting.

- Locating binding poses in protein-ligand systems using reconnaissance metadynamics
  Söderhjelm, P.; Tribello, G. A.; Parrinello, M. *Proc. Nat. Acad. Sci. USA* **2012***, 109*, 5170-5175.
  Abstract:

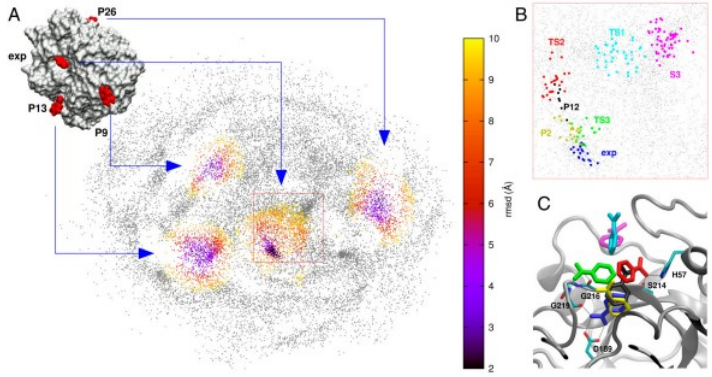

A molecular dynamics-based protocol is proposed for finding and scoring protein-ligand binding poses. This protocol uses the recently developed reconnaissance metadynamics method, which employs a self-learning algorithm to construct a bias that pushes the system away from the kinetic traps where it would otherwise remain. The exploration of phase space with this algorithm is shown to be roughly six to eight times faster than unbiased molecular dynamics and is only limited by the time taken to diffuse about the surface of the protein. We apply this method to the well-studied trypsin-benzamidine system and show that we are able to refind all the poses obtained from a

reference EADock blind docking calculation. These poses can be scored based on the length of time the system remains trapped in the pose. Alternatively, one can perform dimensionality reduction on the output trajectory and obtain a map of phase space that can be used in more expensive free-energy calculations.

- Painting with Biomolecules at the Nanoscale: Biofunctionalization with Tunable Surface Densities
  Schlapak, R.; Danzberger, J.; Haselgrübler, T.; Hinterdorfer, P.; Schäffler, F.; Howorka, S. *Nano Lett.* **2012,** *12*, 1983-1989.
  Abstract:

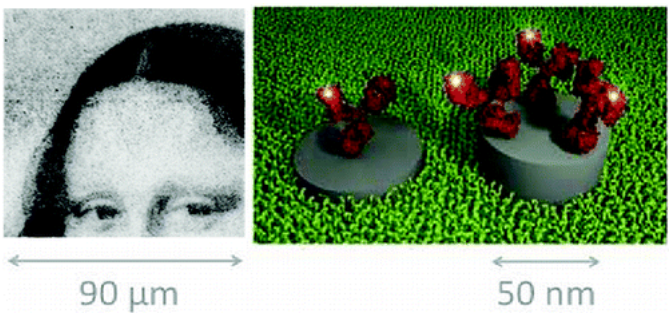

We present a generic and flexible method to nanopattern biomolecules on surfaces. Carbon-containing nanofeatures are written at variable diameter and spacing by a focused electron beam on a poly(ethylene glycol) (PEG)-coated glass substrate. Proteins physisorb to the nanofeatures with remarkably high contrast factors of more than 1000 compared to the surrounding PEG surfaces. The biological activity of model proteins can be retained as shown by decorating avidin spots with biotinylated DNA, thereby underscoring the universality of the nano-biofunctionalized platform for the binding of other biotinylated ligands. In addition, biomolecule densities can be tuned over several orders of magnitude within the same array, as demonstrated by painting a microscale image with nanoscale pixels. We expect that these unique advantages open up entirely new ways to design biophysical experiments, for instance, on cells that respond to the nanoscale densities of activating molecules.

- Nanoparticle-Controlled Aggregation of Colloidal Tetrapods
  Sinkovits, D. W.; Luijten, E. *Nano Lett.* **2011,** *12*, 1743-1748.
  Abstract:

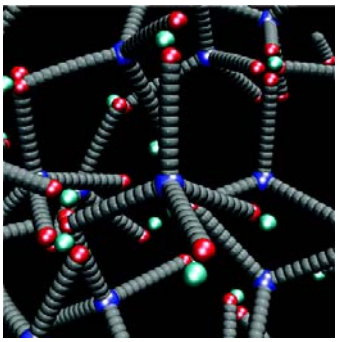

Tetrapods are among the most promising building blocks for nanoscale self-assembly, offering various desirable features. Whereas these particles can be fabricated with remarkable precision, comparatively less is known about their aggregation behavior. Employing a novel, powerful simulation method, we demonstrate that charged nanoparticles offer considerable control over the

assembly of tip-functionalized tetrapods. Extending these findings to tetrapods confined to a gas/liquid interface, we show that regular structures can be achieved even without functionalization.

- Direct Observation of Nanoparticle Superlattice Formation by Using Liquid Cell Transmission Electron Microscopy
  Park, J.; Zheng, H.; Lee, W. C.; Geissler, P. L.; Rabani, E.; Alivisatos, A. P. *ACS Nano* **2012**, *6*, 2078-2085.
  Abstract:

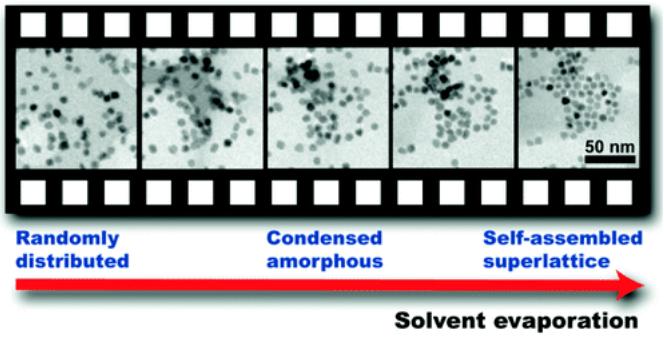

Direct imaging of nanoparticle solutions by liquid phase transmission electron microscopy has enabled unique *in situ* studies of nanoparticle motion and growth. In the present work, we report on real-time formation of two-dimensional nanoparticle arrays in the very low diffusive limit, where nanoparticles are mainly driven by capillary forces and solvent fluctuations. We find that superlattice formation appears to be segregated into multiple regimes. Initially, the solvent front drags the nanoparticles, condensing them into an amorphous agglomerate. Subsequently, the nanoparticle crystallization into an array is driven by local fluctuations. Following the crystallization event, superlattice growth can also occur *via* the addition of individual nanoparticles drawn from outlying regions by different solvent fronts. The dragging mechanism is consistent with simulations based on a coarse-grained lattice gas model at the same limit.

- Chiral Transcription and Retentive Helical Memory: Probing Peptide Auxiliaries Appended with Naphthalenediimides for Their One-Dimensional Molecular Organization
  Pandeeswar, M.; Avinash, M. B.; Govindaraju. T. *Chem. Eur. J.* **2012**, *18*, 4818 – 4822.
  Abstract:

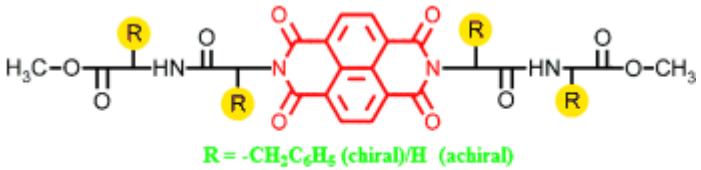

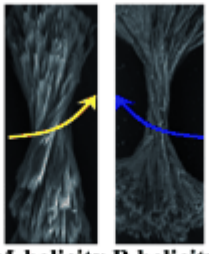

Right or left paradox: Homochiral, heterochiral and achiral peptide auxiliaries appended with naphthalenediimide (NDI, see figure) were employed to demonstrate chiral transcription. We report an interesting phenomenon coined as retentive helical memory. Remarkably, NDI–peptide

conjugates were tuned into hierarchical 1D molecular assemblies of opposite helicity in case of homochiral peptide auxiliaries.

- Synthesis of 2- and 2,7-Functionalized Pyrene Derivatives: An Application of Selective C—H Borylation
  Crawford, A. G.; Liu, Z.; Mkhalid, I. A. I.; Thibault, M.-H.; Schwarz, N.; Alcaraz, G.; Steffen, A.; Collings, J. C.; Batsanov, A. S.; Howard, J. A. K.; Marder, T. B. *Chem. Eur. J.* **2012**, *18*, 5022 – 5035.
  Abstract:

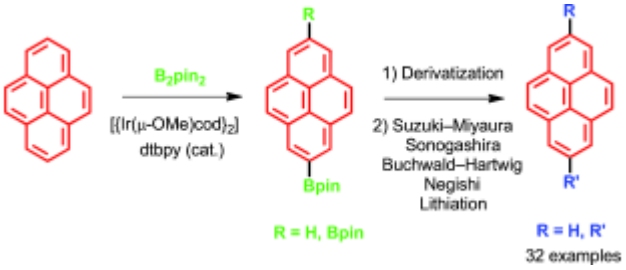

The point of catalytic C—H borylation! Regioselective iridium-catalyzed borylation of pyrene takes place at the 2- and 2,7-positions. The resulting mono- and bisboronate esters can be readily converted into both nucleophilic and electrophilic cross-coupling partners and serve as useful precursors to a wide range of pyrene derivatives of significant photophysical and structural interest, which are otherwise difficult to prepare (see scheme).

- Dithienocyclopentathieno[3,2-*b*]thiophene Hexacyclic Arene for Solution-Processed Organic Field-Effect Transistors and Photovoltaic Applications
  Cheng, Y.-J.; Chen, C.-H.; Lin, T.-Y.; Hsu, C.-S. *Chem. Asian J.* **2012**, 7, 818–825.
  Abstract:

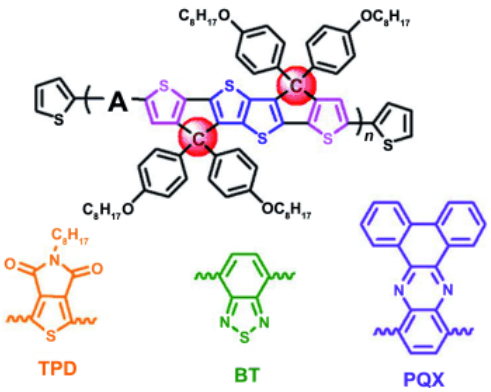

We have developed a ladder-type dithienocyclopentathieno[3,2-*b*]thiophene (**DTCTT**) hexacyclic unit in which the central thieno[3,2-*b*]thiophene ring was covalently fastened to two adjacent thiophene rings through carbon bridges, thereby forming two connected cyclopentadithiophene (**CPDT**) units in a hexacyclic coplanar structure. This stannylated **Sn-DTCTT** building block was copolymerized with three electron-deficient acceptors, dibromo-thieno[3,4-*c*]pyrrole-4,6-dione (**TPD**), dibromo-benzothiadiazole (**BT**), and dibromo-phenanthrenequinoxaline (**PQX**), by Stille polymerization, thereby furnishing a new class of alternating donor–acceptor copolymers: **PDTCTTTPD**, **PDTCTTBT**, and **PDTCTTPQX**, respectively. Field-effect transistors based on **PDTCTTPQX** and **PDTCTTBT** yielded high hole mobilities of 0.017 and 0.053 $cm^2 V^{-1} s^{-1}$, respectively, which are among the highest performances among amorphous donor–acceptor copolymers. A bulk heterojunction solar cell that

incorporated **PDTCTTTPD** with the lower-lying HOMO energy level delivered a higher V_{oc} value of 0.72 V and a power conversion efficiency (PCE) value of 2.59 %.

- New 2, 6-Modified Bodipy Sensitizers for Dye-Sensitized Solar Cells
  Wang, J.-B.; Fang, X.-Q.; Pan, X.; Dai, S.-Y.; Song, Q.-H. *Chem. Asian J.* **2012**, 7, 696–700.
  Abstract:

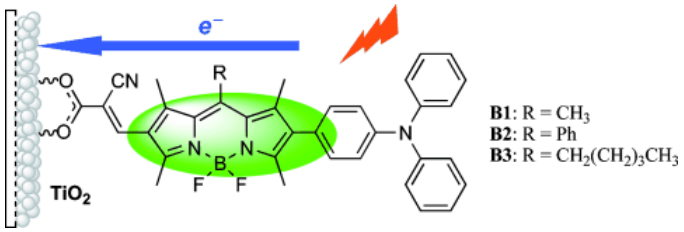

Three novel 2,6-modified Bodipy sensitizers were synthesized and evaluated for their use in dye-sensitized solar cells (DSSCs). Among them, dye **B3**, which carries a *n*-pentyl group at position 8, exhibits the best solar energy conversion efficiency (1.83 %). The results of this study provide a new strategy for the design of Bodipy derivatives as sensitizers for DSSCs.

- Synthesis and Properties of Cycloparaphenylene-2,5-pyridylidene: A Nitrogen-Containing Carbon Nanoring
  Matsui, K.; Segawa, Y.; Itami, K. *Org. Lett.* **2012**, *14*, 1888-1891.
  Abstract:

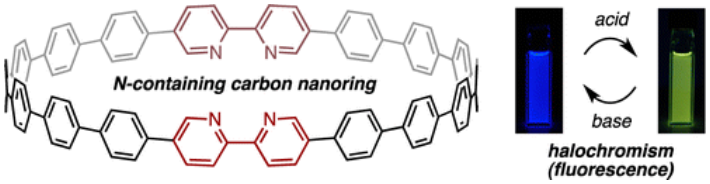

The first synthesis of a nitrogen-containing cycloparaphenylene, cyclo[14]paraphenylene[4]2,5-pyridylidene ([14,4]CPPy), has been achieved. A palladium-catalyzed stepwise assembly of 2,2′-bipyridine, benzene, and L-shaped cyclohexane units, followed by $NaHSO_4$/*o*-chloranil-mediated aromatization, successfully provided [14,4]CPPy. While the absorption and fluorescence properties of [14,4]CPPy were somewhat similar to those of cycloparaphenylenes (λ_{abs} = 344 nm, $\varepsilon = 7.3 \times 10^4$ cm^{-1} M^{-1}, λ_{em} = 427 nm, Φ_F = 0.80), it was found that [14,4]CPPy possesses an interesting halochromic property.

- Photochromic Thienylpyridine–Bis(alkynyl)borane Complexes: Toward Readily Tunable Fluorescence Dyes and Photoswitchable Materials
  Wong, H.-L.; Wong, W.-T.; Yam, V. W.-W. *Org. Lett.* **2012**, *14*, 1862-1865.
  Abstract:

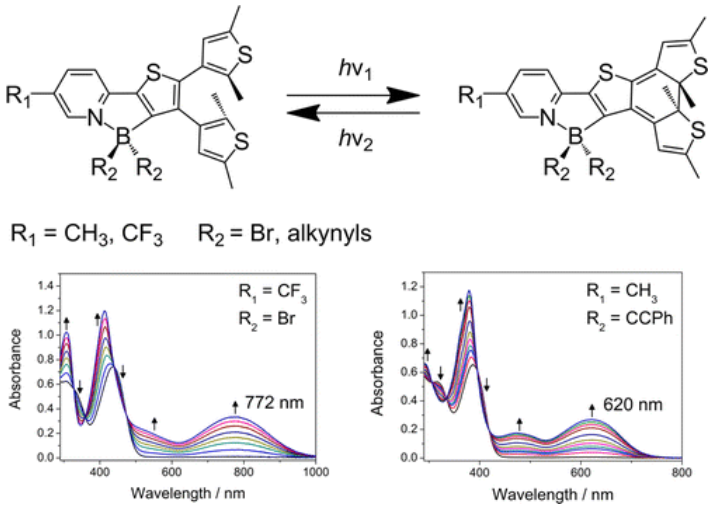

A series of diarylethene-containing N^C chelated thienylpyridine–bis(alkynyl)borane complexes has been designed and synthesized. Their photophysical and photochromic properties have been investigated and presented. The characteristic low-energy absorption band of their closed forms could be readily tuned from the visible range to the near-infrared region.

- Phase behaviour and Janus hierarchical supramolecular structures based on asymmetric tapered bisamide
  Sun, H.-J.; Wang, C.-L.; Hsieh, I-F.; Hsu, C.-H.; Van Horn, R.-M.; Tsai, C.-C.; Jeong, K.-U.; Lotz, B.; Cheng, S. Z. D. *Soft Matter* **2012**, *8*, 4767-4779.
  Abstract:

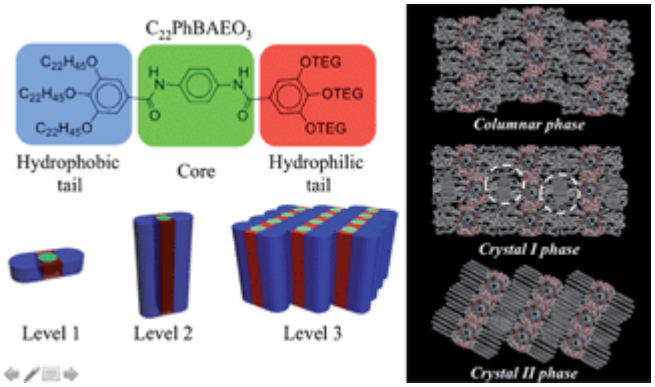

A precisely defined molecular Janus compound based on asymmetric tapered 1,4-bis[3,4,5-tris(alkan-1-yloxy)benzamido] benzene bisamide (abbreviated as $C_{22}PhBAEO_3$) was designed and synthesized, and its phase behavior was fully investigated. The $C_{22}PhBAEO_3$ compound possesses a rigid core with three aromatic rings connected with amide bonds which possess the ability to form hydrogen (H) bonds. Three hydrophobic alkyl flexible tails and three hydrophilic flexible methyl terminated triethylene glycol tails are located at the other end. Major phase transitions and their origins in $C_{22}PhBAEO_3$ were studied *via* DSC and 1D WAXD techniques. Its hierarchical supramolecular crystal structure was further identified through combined techniques of 2D WAXD and SAXS as well as SAED. Results based on computer simulations confirmed the structure determination. It was found that the $C_{22}PhBAEO_3$ possesses three phases through various thermal treatments including a micro-phase separated columnar liquid crystal (*col.*) phase, a metastable *crystal I* phase and a stable *crystal II* phase. Among them, the *crystal II* phase showed that the columnar structure possesses 3D inter-column order and highly crystalline alkyl tails with a long-range overall orientational order. Four

$C_{22}PhBAEO_3$ molecules self-assembled into a phase-separated disc with an ellipsoidal shape having a C_2 symmetry along the disc normal. These discs then stacked on top of each other to generate a 1D asymmetric column through H-bonding, and further packed into a 3D long-range ordered monoclinic lattice. The unit cell parameters of this lattice were determined to be a = 5.08 nm, b = 2.41 nm, c = 0.98 nm, α = 90°, β = 90°, and γ = 70.5°. The alkyl chain tails crystallize within the hydrophobic layers and possess a relatively fixed orientation with respect to the column packing due to the selective interactions based on the hydrophobic/hydrophilic microphase separation. Both phase behaviour and unit cell structure showed significant difference compared with the symmetrically tapered counterparts. The results provided a new approach of fine-tuning not only in the Janus supramolecular structures but also in the formation pathway of the self-assembling process in order to meet the specific requirements for optical and biological applications.

- Thermoresponsive oligoprolines
  Chen, F.; Zhang, X.; Li, W.; Liu, K.; Guo, Y.; Yan, J.; Zhang, A. *Soft Matter* **2012**, *8*, 4869-4872.
  Abstract:

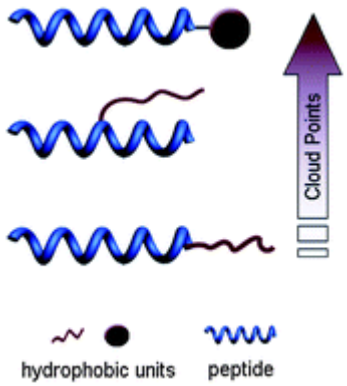

Monodispersed oligoprolines decorated covalently with hydrophobic units show characteristic thermoresponsive behavior with fast and sharp phase transitions at certain concentrations. The phase transition temperatures are dependent on the shape and location of the hydrophobic units, and can be also tuned *via* supramolecular host–guest interactions.